**Article ID:** 1000-324X(2023)03-0343-07 **DOI:** 10.15541/jim20220481

# Effect of High-temperature Annealing on AlN Crystal Grown by PVT Method

YU Ruixian, WANG Guodong, WANG Shouzhi, HU Xiaobo, XU Xiangang, ZHANG Lei

(The State Key Laboratory of Crystal Materials, Institute of Novel Semiconductors, Shenzhen Research Institute of Shandong University, Shandong University, Jinan 250100, China)

**Abstract:** In the process of PVT growth of AlN crystals, there is difficult to maintain ideal thermodynamic equilibrium conditions, causing crystal defects being inevitably generated. High temperature annealing technology has received much attention due to their effectiveness in improving crystal integrity. In this paper, AlN samples grown by PVT method were annealed at high temperature in $N_2$ atmosphere. In order to evaluate the crystalline quality and structural perfection of AlN before and after thermal annealing, high-resolution X-ray diffraction (HRXRD) and Raman spectrum were carried out. In addition, the impurity related band gap changes in the optical properties of AlN crystals were characterized by room temperature photoluminescence (PL) and absorption spectra. The crystal quality of these AlN crystals was significantly improved after annealing at 1400−1800 ℃. The full width at half maximum (FWHM) of the $(10\bar{1}2)$ plane X-ray rocking curve decreased from 104.04 to 79.92 arcsec (1 arcsec=0.01592°) after annealing at 1400 ℃. As the annealing temperature increases, the absorption was significantly enhanced and the band gap became larger, indicating that the annealing process was beneficial to improve the quality of AlN crystals. The results of secondary ion mass spectrometry (SIMS) demonstrate that the annealing process reduces the C impurity, resulting in an increase in band gap of AlN crystal, which is consistent with the results of optical absorption.

**Key words:** high temperature annealing technology; AlN crystal; C impurities; bandgap

With the development of first-generation silicon semiconductor materials and the second-generation GaAs semiconductor materials, the application of its devices has also reached the limit. As a representative of the third-generation semiconductor materials, aluminum nitride (AlN) has the advantages of wide band gap, high critical breakdown electric field, high thermal conductivity, good ultraviolet transmittance and strong radiation resistance[1-3]. Therefore, AlN crystals have broad application prospects in the fields of high-power high-frequency electronic devices and deep ultraviolet light-emitting devices[4-6]. The research of AlN crystals has become a frontier and hot spot in the field of semiconductors. The melting point of the AlN single crystal is very high. The theoretically calculated melting point is 2800 ℃, and the dissociation pressure corresponding to the melting point temperature is as high as 20 MPa. Therefore, it is difficult to grow AlN crystals by melt method under normal pressure. A variety of methods have been developed to grow AlN crystals, including aluminum metal nitridation, solution, hydride vapor phase epitaxy, and physical vapor transport[7-8]. The PVT method has the advantages of simple growth process, fast growth rate, good crystal integrity and high safety, which is the most successful method for growing bulk AlN crytal[9-10].

However, in the process of growing AlN crystals by PVT method, it is difficult to maintain ideal thermodynamic equilibrium conditions, thus crystal defects are inevitably generated, and trace impurities exist in the crucible and raw materials, forming Al vacancies, gap oxygen, and carbon interstitial atoms, *etc*. These defects or vacancies can form midgap energy states in the band gap, which affects the photoexcitation and emission characteristics, hinders band edge transitions, thereby reducing the performance of AlN crystals based deep ultraviolet (DUV) optoelectronic devices[11-13]. Moreover,

**Received date:** 2022-08-13; **Revised date:** 2022-10-09; **Published online:** 2022-11-20
**Foundation item:** Shenzhen Science and Technology Program (JCYJ20210324141607019); Natural Science Foundation of Shandong Province (ZR2022QF044); National Natural Science Foundation of China (52202265)
**Biography:** YU Ruixian (1987–), male, PhD candidate. E-mail: yuruixian0001@126.com
俞瑞仙(1987–), 男, 博士研究生. E-mail: yuruixian0001@126.com
**Corresponding author:** HU Xiaobo, professor. E-mail: xbhu@sdu.edu.cn; ZHANG Lei, associate professor. E-mail: leizhang528@sdu.edu.cn
胡小波, 教授. E-mail: xbhu@sdu.edu.cn; 张 雷, 副教授. E-mail: leizhang528@sdu.edu.cn

these impurities can significantly reduce the transport characteristics such as the carrier mobility of the AlN crystal, thereby limiting its application in microelectronics such as AlGaN based high electron mobility transistor (HEMT). Recently, many methods have been used to reduce defects and impurities to improve crystal quality of AlN by PVT method. Guguschev, *et al*[11] optimized the geometry of the growth device, the raw material purification process and growth parameters to reduce the impurity content of the AlN crystal. Hartmann, *et al*[14] investigated the effects of different supersaturation on the quality and impurity content of AlN crystals. Our research group studied the effects of different temperature gradients on the growth of AlN crystals, and found that the radial temperature gradient was the driving force for expanding the diameter of AlN crystals. However, these reports mainly focus on the effects of growth devices, growth process parameters, *etc*. Further improvements in wafer quality after growth processing have not been investigated. In recent years, it has been reported that high-temperature annealing technique can eliminate the tilt component between the buffer layer grains and realize the reconstruction of AlN, and thus applying to manufacture high-quality, low stress AlN film or efficient DUV-LED device by MOCVD method[12-14]. High temperature annealing technique has received much attention due to its effectiveness in improving the integrity of AlN crystals. However, studies on high temperature annealing of AlN wafers obtained by cutting and polishing AlN boules grown by PVT have not been reported.

To reduce the defects of AlN crystal grown by PVT and the residual stress during subsequent cutting, grinding and polishing, high temperature annealing technique was used to process AlN sample. In this study, the effects of high temperature annealing on the crystal quality, optical properties, stress, and impurity of AlN sample were investigated in detail. It was found that the impurity content of AlN sample decreased under appropriate annealing process, and the crystal quality was significantly improved.

## 1 Experimental

AlN crystals were grown in a home-designed RF-heated furnace with a high purity nitrogen atmosphere by PVT method, and the growth crucible was made of high purity tungsten. The specific growth parameters were described in the literature[15]. The AlN crystals grown by our research group are shown in Fig. 1(a). The grown AlN bulk single crystal was cut into a 500 μm thick sample and then polished. The polished AlN sample is shown in Fig. 1(b). To ensure experimental comparability, the same sample was cut into three small sample and annealed in a high purity nitrogen atmosphere at 1400, 1600 and 1800 ℃, and a schematic view of high temperature annealing process is shown in Fig. 2. These annealed samples were named AlN-1400, AlN-1600 and AlN-1800.

In order to evaluate the crystalline quality and structural perfection of AlN before and after thermal annealing, high-resolution X-ray diffraction (HR-XRD) and Raman spectrum were carried out. In addition, the

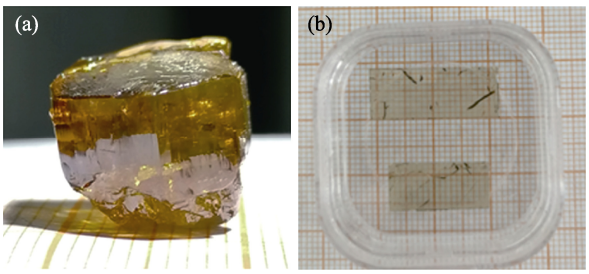


Fig. 1 Photos of AlN crystal sample
(a) Bulk AlN crystal; (b) Polished AlN crystal

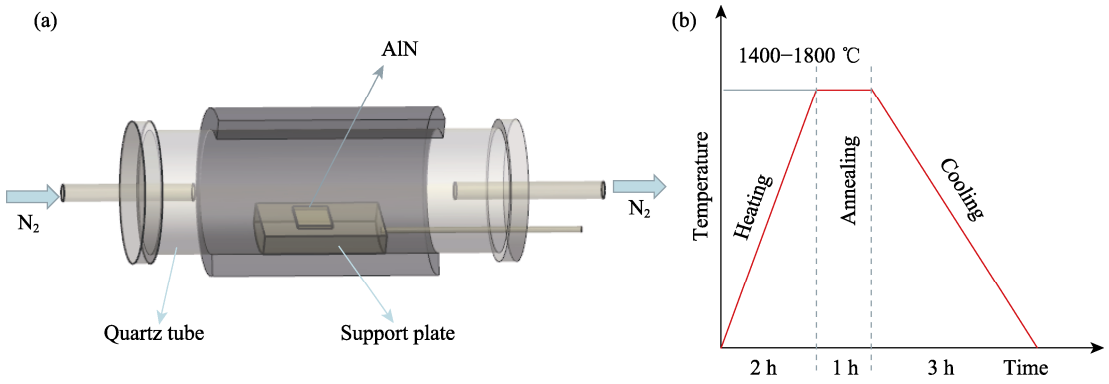


Fig. 2 Schematic view of high temperature annealing process
(a) High temperature annealing furnace; (b) High temperature annealing process

optical properties of the crystals in terms of impurity-related below-bandgap transitions were investigated by room temperature photoluminescence (PL) and absorption spectrum measurements (Varian UV-VIS-NIR cary 50). The Electron backscattered diffraction (EBSD) pattern obtained from the scanning electron microscope (SEM) image was magnified 8000 times. The EBSD maps were acquired by a step size of 500 nm, and the grid was 120×120 points. Secondary ion mass spectroscopy (SIMS) depth profiling was performed using a CAMECA IMS-6f with a 50 nA Cs+beam over a 180 μm × 180 μm area.

## 2　Results and discussion

EBSD is an effective method to characterize crystal orientation, the plastic strain existing in the lattice and related information in crystal materials. The EBSD measurement is performed on the AlN without annealing to determine its crystal orientation and crystal quality. Fig. 3(a) is a Kikuchi diffraction pattern of the AlN sample. As seen from the figure, AlN sample has a highly oriented crystal structure along the $(11\bar{2}0)$ direction, and the pole figure (Fig. 3(c)) also proves that the crystal is in the $(11\bar{2}0)$ direction. Fig. 3(b) shows the band slope (BS) of an AlN crystal from EBSD mapping data. The mapped colors concentrate in a mixture of green and yellow, indicating that the BS value changes by less than 75. These results indicate that the AlN sample without annealing have a high crystallographic integrity.

The quality of AlN crystals without and with annealing are characterized by high-resolution X-ray diffraction (HRXRD) rocking curves (Fig. 4). According to the relationship between the Burger's vector and the XRD Bragg peak width, the threading dislocations in the AlN crystal are dominated by pure edge type dislocations. Therefore, the FWHM of the $(10\bar{1}2)$ plane can directly reflect the AlN crystal quality. Table 1 is the FWHM of the $(10\bar{1}2)$ plane of symmetry $\omega$-scan of the AlN crystal without and with annealing, and the FWHM value (80, 79 and 97 arcsec at 1400, 1600, and 1800 ℃, respectively) of the $(10\bar{1}2)$ plane of the annealing sample is

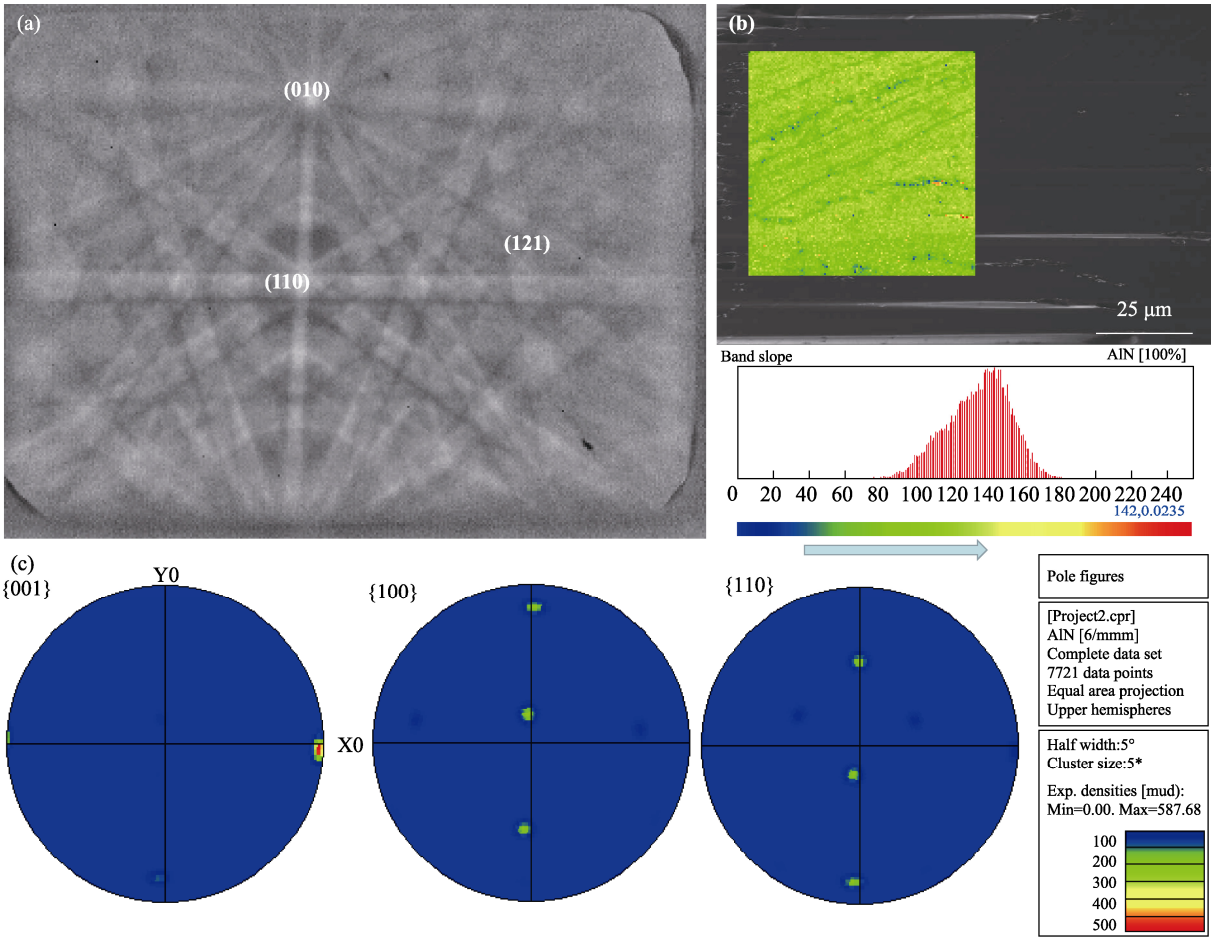


Fig. 3　EBSD of AlN crystal sample

(a) EBSD Kikuchi patterns of AlN crystal without annealing; (b) Band slop obtained from EBSD mapping date; (c) Pole figures of AlN without annealing

significantly lower than that of the sample without annealing (104 arcsec). The edge dislocations density($\rho_e$) can be calculated by the following formula:

$$\rho_e = \frac{\beta^2_{(10\bar{1}2)}}{2\pi \ln 2 \times |b_a|^2} \quad (1)$$

Where $\beta$ is the FWHM of planes, $|b_a|$ is the Burgers vector lengths equated to $a$-axial lattice constants. Table 1 is the calculated dislocation density. It can be seen from the table that the dislocation density of the sample after high temperature annealing is reduced to some extent. The AlN sample annealed at 1400 ℃ has the lowest dislocation density, a 41% reduction, as compared to the sample without annealing. During the annealing process, the higher $N_2$ background gas pressure makes the transport of other substances to the surface of AlN less, and the atoms on the surface of AlN are mainly migrated and recombined. When the annealing temperature is moderate (1400–1600 ℃), Al atoms and N atoms have enough activity, and some of Al atoms and N atoms will migrate to the original vacancies and defects, thus reducing point defects and line defects. When the annealing temperature is too high (1800 ℃), Al atoms and N atoms have very high activity, and the atoms on the AlN surface will migrate disorderly, instead of reducing the dislocation. FWHM of the sample annealed at 1600 ℃ is almost the same as that at 1400 ℃ (80 arcsec), thus 1400–1600 ℃ is the optimum annealing temperature range.

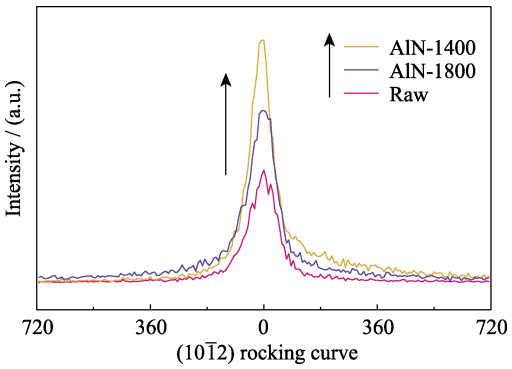


Fig. 4 XRD $\omega$-scan rocking curves of AlN (10$\bar{1}$2) diffractions

**Table 1 Calculated edge dislocations density($\rho_e$) of AlN samples**

| Sample | (10$\bar{1}$2) FWHM/arcsec* | Edge dislocations density, $\rho_e$/($\times 10^7$, cm$^{-2}$) |
|---|---|---|
| Raw | 104.04 | 5.80 |
| AlN-1400 | 79.92 | 3.42 |
| AlN-1600 | 78.92 | 3.34 |
| AlN-1800 | 97.2 | 5.06 |

Raman spectroscopy is an effective method for evaluating crystal structure, quality, and residual stress. Fig. 5 shows the Raman spectra of AlN samples without and with annealing at different temperatures. It can be observed that there are four peaks $E_2$ (low), $A_1$ (TO), $E_2$ (high) and $E_1$ (TO) associated with the (11$\bar{2}$0) plane of wurtzite structure AlN. The in-plane residual stress ($\sigma_a$) can be derived by using Eq. (2):

$$\sigma_a = k^{-1}\Delta\omega \cdot [E_2(\text{high})] \quad (2)$$

Where $\Delta\omega \cdot [E_2(\text{high})]$ is the strain-induced Raman frequency shift for $E_2$(high) mode and the biaxial stress coefficient $k$ roughly equals to 2.4 cm$^{-1}$·GPa$^{-1}$. The $E_2$(high) mode peaks of the AlN samples without and with annealing all locate at 656.23 cm$^{-1}$, which coincides well with the reported value (657.4 cm$^{-1}$) of freestanding AlN crystal. These results indicate that the stress value of the small-sized AlN sample obtained by homo-epitaxial reaches the minimum, and the effect of high-temperature annealing on small-sized sample stress is small. However, the impact on the stress of large-sized AlN samples remains to be further studied.

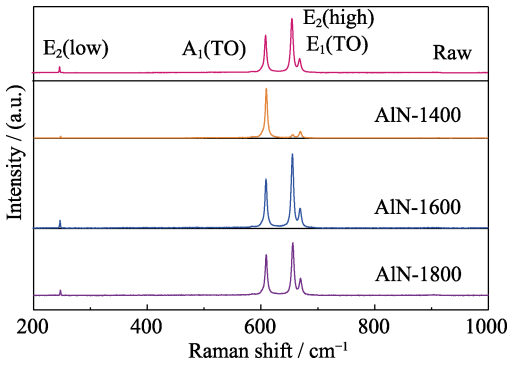


Fig. 5 Raman spectra of AlN samples without and with annealing at different temperatures

Fig. 6 shows the optical absorption spectra of the AlN crystals with and without annealing. There is an obvious absorption peak at 634 nm (1.96 eV) with inset in Fig. 6(a). The strong absorption peak of the AlN crystal at 634 nm (1.96 eV) may be due to the defect energy levels formed by carbon and oxygen.

Significant enhancement of absorption is observed with annealing temperature increasing, indicating that the annealing process is beneficial to improve the quality of AlN crystal. The relationship of the molar absorption coefficient($\alpha$) and photon energy($E$) is listed below:

$$\alpha h\upsilon = B(h\upsilon - E_g)^m \quad (3)$$

Where $B$ is the proportional constant, $E_g$ is the optical band gap of semiconductor material, and the value of $m$ is related to semiconductor material and transition type.

When $m$=1/2, it corresponds to the dipole transition allowed by direct bandgap semiconductors. By Lamber-bier's law:

$$A = \alpha bc \tag{4}$$

Where $b$ is sample thickness, $c$ is concentration, where $bc$ is a constant, if $B_1=(B/bc)^{1/2}$, Then formula (3) can be written:

$$(AE)^2 = B_1(E - E_g) \tag{5}$$

According to the correlation curves of $(\alpha E)^2$ and $E$, as shown in Fig. 6(b), the band gap of AlN with annealing is higher than that without annealing. The band gaps are 3.90, 3.93, 3.91, and 4.05 eV for the AlN without and with annealing at 1400, 1600, and 1800 ℃. The variation trend of the band gap is shown in the inset in Fig. 6(b). The band gap values of the samples are all smaller than the theoretical band gap value of AlN, which may be due to crystal defects or impurities induced intermediate levels associated with the conduction band resulting in a decrease in band gap[16]. The deep ultraviolet absorption coefficient of AlN crystals mainly depends on the impurities C and O[9,17]. According to density functional theory calculations and experiments, it is shown that C impurities exist in the form of CN in AlN crystals, resulting in a very strong ultraviolet absorption peak at about 265 nm (4.7 eV)[18]. The C mainly comes from the graphite insulation. The possible gas phase substances are CN, CO or $C_xH_y$. The recombination of $V_{Al}$ and O impurity defects leads to absorption at 280–380 nm (3.3–4.3 eV)[19]. O is mainly vapor-phase $Al_2O$ sublimed from raw materials at the growth interface, and is affected by factors such as the raw material particle size, sintering process, and purity of the chamber. Therefore, AlN crystals with high UV transmittance can be obtained by suppressing and eliminating the content of C and O impurities. The band gap increases from 3.90 eV for AlN crystal without annealing to about 4.05 eV for AlN crystal with annealing at 1800 ℃. The increase in band gap is attributed to the reduction of defects and impurities[20], which confirms that high temperature annealing improves the crystal quality of the AlN sample.

The impurity incorporation in the AlN crystals is characterized by SIMS. As shown in Fig. 7, three main impurities of silicon, carbon and oxygen are detected in the AlN crystals. The carbon mainly comes from the graphite insulating, and the silicon and oxygen elements are mainly derived from the AlN raw material. The silicon concentration of the AlN samples without and with annealing at 1600 ℃ is $1\times10^{17}$ $cm^{-3}$ without substantial change. After annealing, the carbon concentration decreases from $2.5\times10^{19}$ to $2.0\times10^{19}$ $cm^{-3}$, and the oxygen concentration increases from $3.1\times10^{19}$ to $3.5\times10^{19}$ $cm^{-3}$. In this experiment, intermediate frequency heating and graphite insulation system are used. C mainly comes from the graphite insulation in the growth equipment, thus it is inevitable that the C concentration is relatively high. O is mainly the gas phase $Al_2O_3$ sublimated from AlN raw material at the growth interface. At present, the inhibition and elimination of C and O impurities are in progress. The decrease of carbon concentration may result in an increase in the band gap of the AlN crystal, which is consistent with the optical absorption results. The increase of oxygen concentration after annealing may lead to the enhanced absorption of AlN crystals at 634 nm (1.96 eV). The increase of oxygen concentration after annealing may be attributed to the residual of the insulating material, and a higher purity insulating material is used in subsequent experiments.

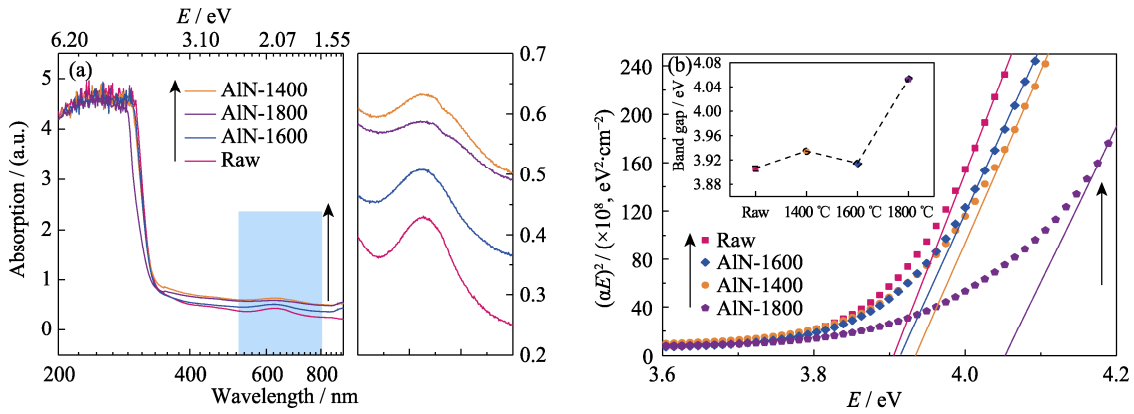


Fig. 6　Optical absorption spectra of the AlN crystals with and without annealing

(a) Absorption spectra of the AlN without and with annealing at different temperatures with right enlarged spectra showing an absorption peak at 634 nm; (b) Correlation curves of $(\alpha E)^2$ on $E$ with inset showing the band gap of AlN without and with annealing at different temperatures

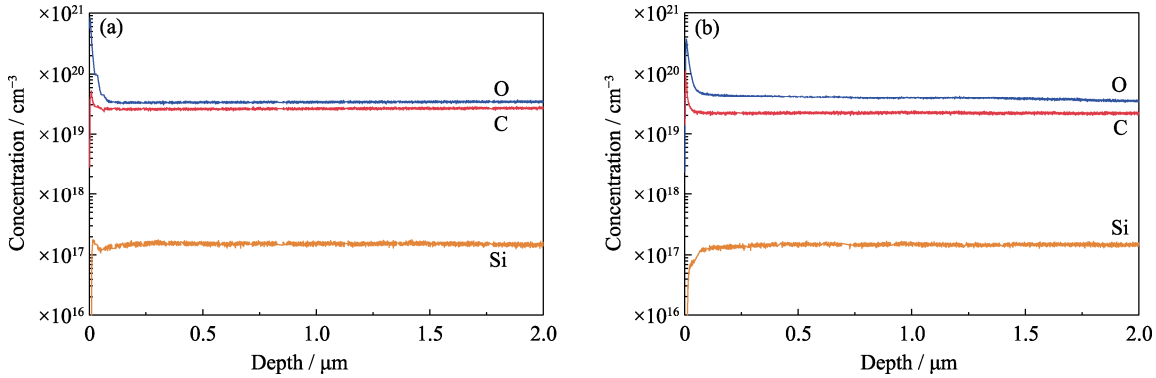


Fig. 7 SIMS depth profiles of AlN crystal without (a) and with annealing at 1600 ℃ (b)

## 3 Conclusions

In conclusion, AlN crystals grown by the PVT method were annealed in the temperature range of 1400 ℃ to 1800 ℃ under nitrogen atmosphere. The crystal quality of these AlN crystals was improved significantly after thermal annealing. The minimum FWHM of $(10\bar{1}2)$ is 79.92 arcsec after annealed at 1400 ℃. SIMS measurements show that the thermal annealing process reduces C impurities. The band gap increases from 3.90 eV (unannealed AlN crystal) to about 4.05 eV (1800 ℃-annealed AlN crystal). The increase in the band gap is attributed to the reduction of defects and impurities, further demonstrating the improved crystal quality. From these results, it is concluded that the high temperature annealing technique can effectively improve the quality of AlN crystals.

## References:

[1] SUN M S, LI J F, ZHANG J C *et al*. The fabrication of AlN by hydride vapor phase epitaxy. *Journal of Semiconductors*, 2019, **40:** 121803.

[2] YU R X, LIU G X, WANG G D *et al*. Ultrawide-bandgap semiconductor AlN crystals: growth and applications. *J. Mater. Chem. C*, 2021, **9:** 1852.

[3] YU R X, CHEN C M, ZHANG L *et al*. Influence of different heater structures on the temperature field of AlN crystal growth by resistance heating. *Materials*, 2021, **14:** 7441.

[4] ZHENG W, HUANG F, ZHENG R S, *et al*. Low-dimensional structure vacuum-ultraviolet-sensitive ($\lambda$<200 nm) photodetector with fast-response speed based on high-quality AlN micro/nanowire. *Adv. Mater.*, 2015, **27:** 3921.

[5] CHEN Z L, LIU Z Q, WEI T B, *et al*. Improved epitaxy of AlN film for deep-ultraviolet light-emitting diodes enabled by graphene. *Adv. Mater.*, 2019, **31:** 1807345.

[6] LU T J, LIENHARD B, JEONG K Y, *et al*. Bright high-purity quantum emitters in aluminum nitride integrated photonics. *ACS Photonics*, 2020, **7:** 2650.

[7] LIU X H, ZHANG J C, SU X J, *et al*. Fabrication of crack-free AlN film on sapphire by hydride vapor phase epitaxy using an *in situ* etching method. *Appl. Phys. Exp.*, 2016, **9:** 045501.

[8] KATAGIRI Y, KISHINO S, OKUURA K, *et al*. Low-pressure HVPE growth of crack-free thick AlN on a trench-patterned AlN template. *J. Cryst. Growth*, 2009, **311:** 2831.

[9] HARTMANN C, DITTMAR A, WOLLWEBER J, *et al*. Bulk AlN growth by physical vapor transport. *Semicond. Sci. Technol.*, 2014, **29:** 084002.

[10] ZHUANG D, HERRO Z G, SCHLEAAER R, *et al*. Seeded growth of AlN single crystals by physical vapor transport. *J. Cryst. Growth*, 2006, **287:** 372.

[11] GUGUSCHEV C, DITTMAR A, MOUKHINA E, *et al*. Growth of bulk AlN single crystals with low oxygen content taking into account thermal and kinetic effects of oxygen-related gaseous species. *J. Cryst. Growth*, 2012, **360:** 185.

[12] TANIYASU Y, KASU M, MAKIMOTO T. Electrical conduction properties of n-type Si-doped AlN with high electron mobility (>100 $cm^2 \cdot V^{-1} \cdot s^{-1}$). *Appl. Phys. Lett.*, **2004, 85:** 4672.

[13] STRASSBURG M, SENAWIRATNE J, DIETZ N. The growth and optical properties of large, high-quality AlN single crystals. *J. Appl. Phys.*, 2004, **96:** 5870.

[14] HARTMANN C, WOLLWEBER J, DITTMAR A, *et al*. Preparation of bulk AlN seeds by spontaneous nucleation of freestanding crystals. *Jpn. J. Appl. Phys.*, 2013, **52:** 08JA06.

[15] WANG G D, ZHANG L, WANG Y, *et al*. Effect of temperature gradient on AlN crystal growth by physical vapor transport method. *Cryst. Growth Des.*, 2019, **19:** 6736.

[16] MOTAMEDI P, CADIEN K. Structural and optical characterization of low-temperature ALD crystalline AlN. *J. Cryst. Growth*, 2015, **421:** 45.

[17] HARTMANN C, MATIWE L, WOLLWEBER J, *et al*. Favorable growth conditions for the preparation of bulk AlN single crystals by PVT. *CrystEngComm*, 2020, **22:** 1762.

[18] COLLAZO R, XIE J, GADDY B, *et al*. On the origin of the 265 nm absorption band in AlN bulk crystals. *Appl. Phys. Lett.*, 2012, **100:** 191914.

[19] GADDY B E, BRYAN Z, BRYAN I, *et al*. The role of the carbon-silicon complex in eliminating deep ultraviolet absorption in AlN. *Appl. Phys. Lett.*, 2014, **104:** 202106.

[20] ZHAO L, YANG K, AI Y J, *et al*. Crystal quality improvement of sputtered AlN film on sapphire substrate by high-temperature annealing. *J. Mater. Sci.: Mater. Electron.*, 2018, **29:** 13766.

# 高温退火对 PVT 法生长的 AlN 晶体质量的影响

俞瑞仙, 王国栋, 王守志, 胡小波, 徐现刚, 张 雷

(山东大学 深圳研究院, 新一代半导体材料研究院, 晶体材料国家重点实验室, 济南 250100)

**摘 要:** 在 PVT 法生长 AlN 晶体的过程中, 很难保持理想的热力学平衡状态, 不可避免地会产生晶体缺陷。高温退火技术对提高晶体完整性十分有效，受到了广泛关注。本工作在 $N_2$ 气氛环境下对 PVT 法生长的 AlN 晶片进行高温退火研究。为了评价退火前后 AlN 晶体的质量和结构变化情况, 进行了高分辨率 X 射线衍射(HRXRD)和拉曼光谱分析。通过室温光致发光(PL)和吸收光谱对 AlN 晶体的光学性质以及与杂质相关的带隙变化情况进行了表征。在 1400~1800 ℃退火后, AlN 晶体质量显著提高。1400 ℃退火后, (10-12)晶面的 X 射线摇摆曲线的半峰宽(FWHM)从 104.04 arcsec 减小到 79.92 arcsec。随着退火温度升高, 吸收性能明显增强, 带隙增大, 说明高温退火处理有利于提高 AlN 晶体的质量。二次离子质谱(SIMS)结果表明, 退火过程降低了 C 杂质, 增加了 AlN 晶体的带隙, 这与光吸收结果一致。

**关　键　词:** 高温退火技术; AlN 晶体; C 杂质; 带隙

**中图分类号:** TB34　　**文献标志码:** A